



On the Dynamic Behavior of a Liquid Droplet Impacting upon a Wall Having Obstacles

B. Kang

Department of Mechanical Engineering, Chonnam National University., 77 Yongbong-ro, Buk-gu, Gwangju, Korea

Corresponding Author Email: bskang@jnu.ac.kr

(Received May 23, 2014; accepted August 31, 2014)

ABSTRACT

In this paper, the effects of a step edge and a stationary droplet on the dynamic behavior of a droplet impacting upon a wall are experimentally studied. The main parameters were the distance from the step edge to the center of the impacting droplet and the center-to-center distance between the stationary and impacting droplets. Photographic images showed the coalescence dynamics, shape evolution and contact line movement of the impacting droplet. The spread length is presented for the step edge and two coalescing droplets. The droplets exhibited much different dynamic behavior depending on the location of the step edge. The momentum of the impacting droplet was better transferred to the stationary droplet as the center-to-center distance between the two droplets was reduced, resulting in more spreading of the coalescing droplet.

Keywords: Coalescence; Impacting droplet; Stationary droplet; Step edge.

NOMENCLATURE

D_o	diameter of an impacting droplet	L_r	length from the center of a stationary droplet to the right end of a merging droplet
D_s	diameter of a stationary droplet	L_t	total length of a merging droplet
H	height of a step edge	V	speed of an impacting droplet
L_1	distance between a step edge and the center of an impacting droplet	μ	viscosity of liquid
L_2	distance between impacting and stationary droplets	ρ	density of liquid
L_l	length from the center of an impacting droplet to the left end of a merging droplet	σ	surface tension of liquid

1. INTRODUCTION

The characteristics of sprays impacting on a rigid surface are of great importance in many technical applications including spray cooling, spray painting, fuel injection in combustion engines, inkjet printing, spray forming, and fire extinguishing by sprinklers (Crowe et al. 1998, Lefebvre 1989). In internal combustion engines, the impact behavior of fuel sprays on a wall, which affects the rate of fuel evaporation and droplet distribution, is commonly observed. Many researches on a single droplet impacting a surface have been conducted to understand the characteristics of impacting sprays from a microscopic point of view (Chandra and Avedisian 1991, Mundo et al. 1995, Rioboo et al. 2002). Rein (1993), Yarin (2006), and Moreira et al. (2010) provided comprehensive information on this subject.

A droplet impacting a surface shows extremely

complex phenomena according to parameters such as droplet size, droplet velocity, surface condition, incident angle, fluid properties, and if present, liquid film thickness and gas boundary layer. Some examples of these phenomena, clarified by Bai and Gossman (1995), include sticking, spreading, rebounding, rebounding with breakup, boiling-induced breakups, breakups, and splashing. Despite these studies, however, our understanding of these phenomena remains very limited.

In addition, there has been little study on how the behavior of an impacting droplet is influenced by some obstacles or stationary droplets existing around the impacting droplet. Such situations are easily encountered in real applications. Jossierand et al. (2005) performed experimental and numerical analyses about the phenomenon in which an impacting droplet spreads as a liquid film around an obstacle, changing the height of the obstacle by building up a bonding tape layer. Bussmann et al.

(1999) performed a numerical analysis of a liquid droplet falling on a step edge of 1 mm height, and compared the results with the experimental results.

The deposition of liquid droplets (molten metal, polymer, or molten wax) on a solid surface has been applied in inkjet printing, microforming, rapid molding, and electronic packaging, etc. In these fields of application, it is important to accurately connect the desired lines or patterns by correctly positioning the liquid droplets. If adjacent liquid droplets touch each other, however, the flow between the droplets by surface tension can cause the lines to become disconnected or the line thickness to become irregular. Such phenomenon is very difficult to analyze.

Many studies on the coalescence phenomenon between adjacent liquid droplets have been conducted. Menchaca-Rocha et al. (2001) studied droplet shape changes by combining two mercury liquid droplets on a glass surface. They observed that the neck portion of the coalescing droplets followed the $t^{1/2}$ law well, where t is time. Ristenpart et al. (2006) studied the coalescence phenomenon between two liquid droplets on a high hydrophilic surface, and showed that the changes of the neck widths of the coalescing droplets exponentially increased with time. Thoroddsen et al. (2005) investigated the coalescence of a stationary droplet with a pendant droplet on a surface. Andrieu et al. (2002) conducted experiments and theoretical analysis on the coalescence phenomenon of water droplets on a surface where they grow by condensation and eventually touch each other and coalesce.

Most of these studies reported that only the effects of surface tension and viscosity are dominant owing to the low inertial force. In actual applications, however, the effects of the inertial force between the coalescing droplets, the hydrophilic property of the surface, and the drop interval between liquid droplets are very important. For the inertia-dominant situation, Roisman et al. (2002) established a droplet coalescence model corresponding to the case in which the Re and We numbers were high and the interaction between the liquid droplets was small. The results of the model well matched the experimental results. Li et al. (2010) measured the maximum and minimum spreading lengths by experiments in which the behavior of the impacting droplet coalescing with a stationary droplet was observed. From the results, they proposed an experimental correlation equation that could predict these lengths.

This paper aims to improve our understanding of the dynamic behavior of a droplet impacting a surface having different kinds of obstacles such as a step edge and a stationary droplet. These obstacles disturb the spreading-contraction process of the impacting droplet on the solid surface. We visualized the dynamic behavior of an impacting droplet by time-delayed photography. The effects of the obstacles were analyzed by measuring the various lengths of the spreading-contracting liquid droplet. For the case of the step edge as the

obstacle, the distance between the impacting droplet and the step edge was varied in the experiments. For the case of a stationary droplet as the obstacle, a liquid droplet impacts around a stationary droplet and merges with it. We investigated the variations of the shape and lengths of the coalescing droplet according to the distance between the impacting droplet and the stationary droplet.

2. EXPERIMENTAL APPARATUS AND CONDITIONS

The experiments in which a liquid droplet impacts near a step-type edge and those in which a liquid droplet merges with a stationary droplet are schematically shown in Figs. 1 and 2, respectively. D_o and D_s are the diameters of the impacting and stationary droplets, respectively, and V is the speed of the impacting droplet. H is the height of the step edge, L_1 is the distance between the step edge and the center of the impacting droplet, and L_2 is the distance between the impacting and stationary droplets. L_l is the length from the center of the impacting droplet to the left end of the merging droplet, L_r is the length from the center of the stationary droplet to the right end of the merging droplet, and L_t indicates the total length of the merging droplet.

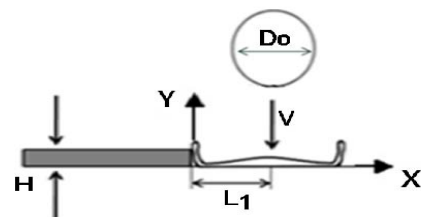


Fig. 1. A liquid droplet impacting near a step-type edge.

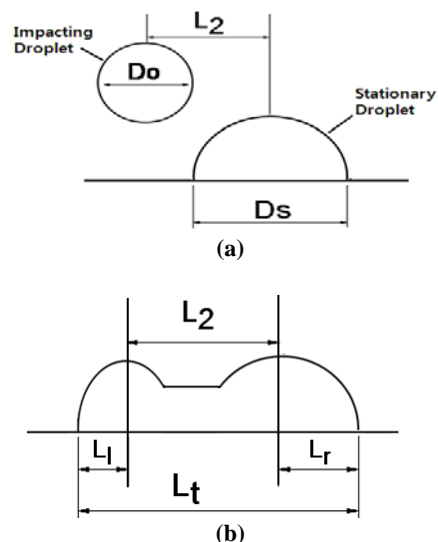


Fig. 2. A liquid droplet merging with a stationary droplet (a) before impact (b) after impact.

In order to visualize the collision behavior of a liquid droplet on a flat surface, time delayed photography was used. Time delayed photography

takes time sequential photographs of desired phenomena at delayed time moments from a reference moment. Figure 3 shows the schematic diagram of the experimental setup constructed to record the deformation behavior of a single droplet impacting a surface having an obstacle. The setup consists of the test surface, the time delayed photography system, and the droplet generating system. The test surface was made of Aluminum. Fluid(water) was supplied from a syringe pump to a needle. The ID and OD of the needle for the step edge experiments were 0.394 and 0.711 mm, respectively, and those for coalescing experiments with a stationary droplet were 0.292 and 0.559 mm, respectively.

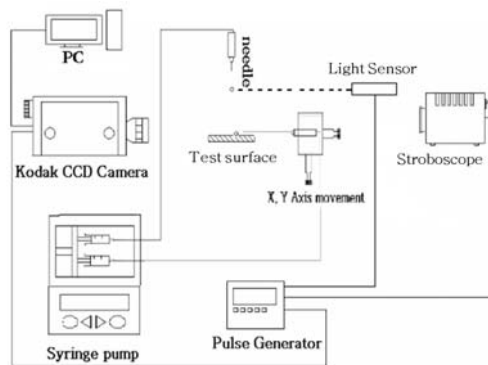


Fig. 3. The schematic diagram of the experimental setup.

A small droplet made to hang on the sharp tip of the needle gradually became larger, separated from the tip of the needle and fell a given distance before impacting the surface. When the optical sensor senses a falling droplet and sends a signal to the pulse generator, the pulse generator then sends a signal to the CCD camera and to the stroboscope after a pre-set desired delay time. Then, droplet images of the behavior of the impacting droplet are taken in time sequence. The droplets impacted an aluminum plate, and the height of the step edge was $H = 0.1$ mm.

The experimental conditions are shown in Table 1. The velocity and diameter of the impacting droplet were calculated by analyzing two images that were taken just before the impact. The diameter of the droplet corresponding to the total area covered by the droplet before impact was calculated. The velocity of the droplet was obtained by dividing the distance travelled by the droplet by the time it took for the droplet to travel that distance. The We and Re numbers are defined as $\rho D_o V^2 / \sigma$ and $\rho V D_o / \mu$, respectively, based on the liquid properties instead of gas properties. For the contact angle of water droplets ($D=3.0$ mm) on the aluminum surface, we used $\theta=63.4^\circ$ obtained from the results of Jin et al. (2012). In the impact experiments with a step edge, the distances between the droplet and the step edge were $L_1 = -3, 0, +3$ mm, respectively. In the experiments where the droplet merged with a stationary droplet, the distances between the impacting and stationary droplets were $L_2 = 4.5,$

$3.0, 1.5$ mm, respectively.

Table 1 Experimental conditions

Case	L_1, L_2 (mm)	V (m/s)	D_o (mm)	$We = \rho D_o V^2 / \sigma$	$Re = \rho V D_o / \mu$
Step edge experiment					
1	$L_1 = -3.0$	2.9	3.5	410	10,260
2	$L_1 = 0$	2.9	3.5	410	10,260
3	$L_1 = 3.0$	2.9	3.5	410	10,260
Coalescence experiment					
4	$L_2 = 4.5$	3	3.1	381	9,260
5	$L_2 = 3.0$	3	3.1	381	9,260
6	$L_2 = 1.5$	3	3.1	381	9,260

3. RESULTS AND DISCUSSION

3.1 Impact Experiments with a Step Edge

A liquid droplet impacting a solid surface quickly spreads by the inertial force in the early stage. Some of the energy of the droplet is dissipated by the internal flow of the droplet and the rest is converted to surface energy to form the interfaces between the droplet and air and between the droplet and the solid surface, while the surface tension force acts as the dominant force. Then, the droplet repeatedly spreads and contracts with gradually decreasing speed, until it reaches the final state at which all of the kinetic energy of the liquid droplet is dissipated.

Figures 4 through 6 show the behavior of the impacting droplet near a step edge for distances of $L_1 = -3, 0, +3$ mm, respectively. For the case of $L_1 = -3$ mm (Fig. 4), the fore-end of the right side of the spreading-contraction droplet does not contact the solid surface, so there is no frictional force between the droplet and the surface. In other words, the left side of the spreading-contraction droplet is hindered in the spreading-contraction process by the surface frictional force, but the fore-end of the right side is not hindered. This can be verified in the photographic images, which show the asymmetry between the left and right sides. In addition, the liquid film is not falling down the step edge wall due to the inertial and surface tension forces in the spreading-contraction process.

For the case of $L_1 = 0$ mm (Fig. 5), the liquid droplet impacts just on the center of the edge. The droplet almost separates to both sides in the spreading process by the edge, but it coalesces again in the contraction process. Generally, the left-right symmetric properties are maintained well. For the case of $L_1 = +3$ mm (Fig. 6), the droplet impacts the lower right solid surface of the step edge. The spreading process of the left side of the droplet is hindered by the step edge wall, and the liquid film climbs up the edge wall. Small droplets are separated from the left edge of the liquid film.

The variation of the diameter of the spreading-contracting droplet with time is shown in Fig. 7

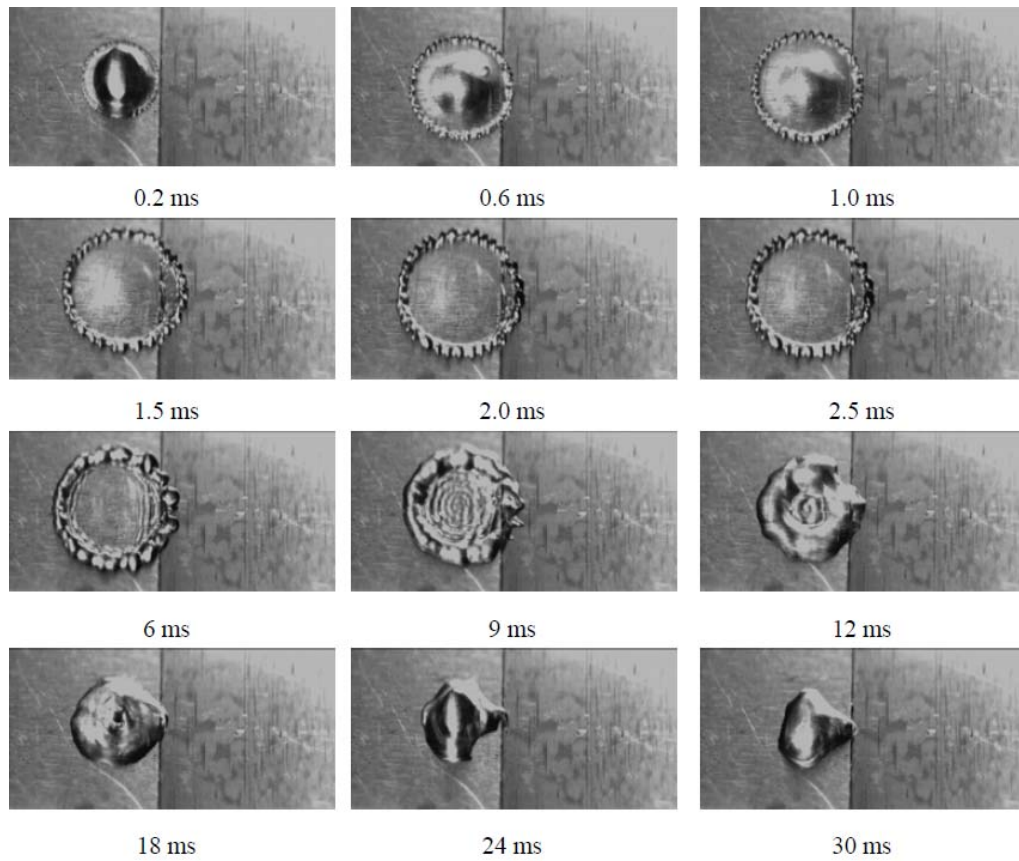


Fig. 4. The behavior of the impacting droplet near a step edge for distance of $L_1 = -3$ mm.

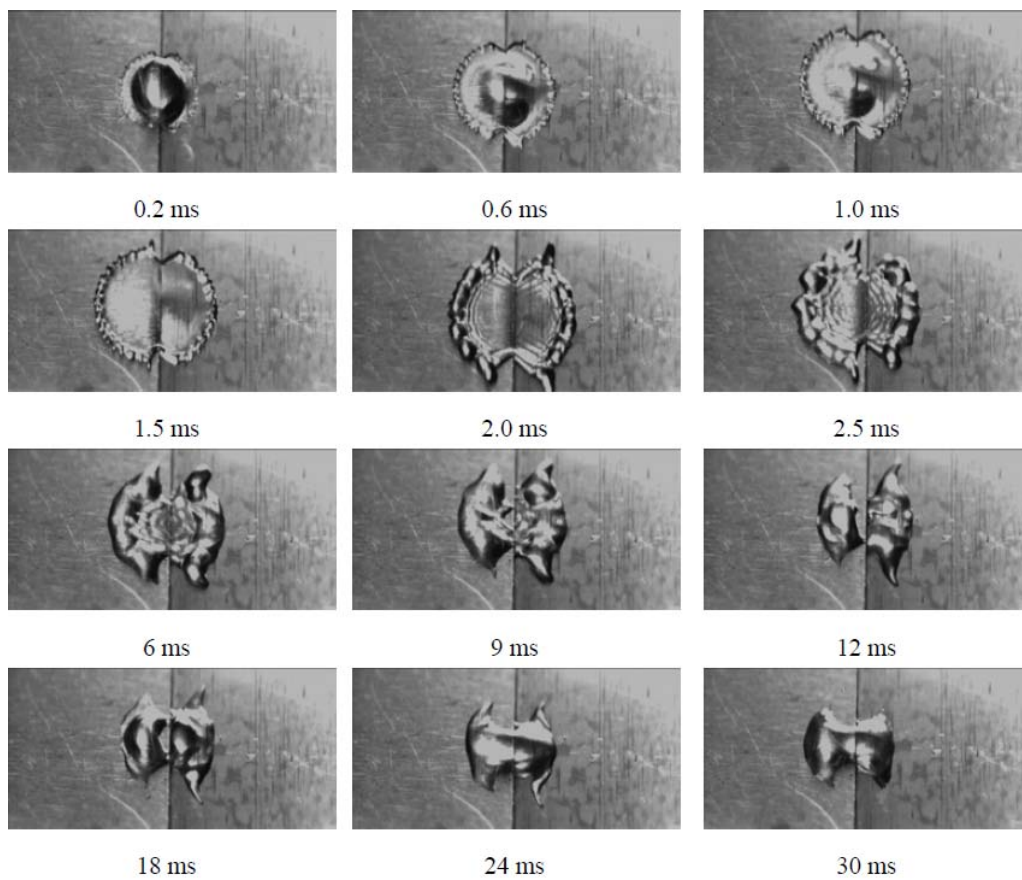


Fig. 5. The behavior of the impacting droplet near a step edge for distance of $L_1 = 0$ mm.

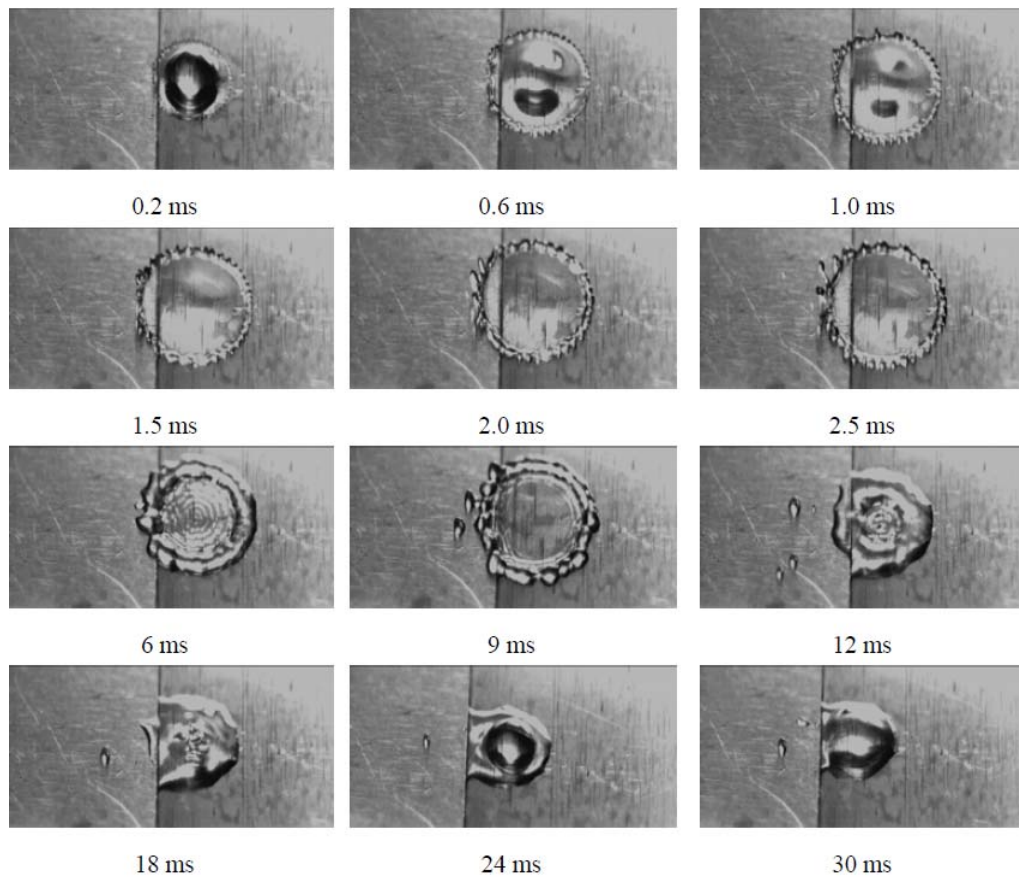


Fig. 6. The behavior of the impacting droplet near a step edge for distance of $L_1 = +3$ mm.

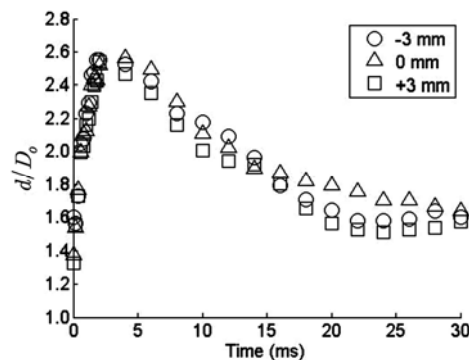


Fig. 7. The time history of the diameter of the spreading-contracting droplet.

The diameter is the length from the left end to the right end of the spreading-contracting droplet in the images. If we assume errors of ± 2 pixels in measuring the length of the diameter from the droplet images, the error of the diameter measurement (d) becomes ± 0.1 mm by the conversion factor, and the non-dimensionalized value of it (d/D_0) is ± 0.03 .

In the early stage of the spreading process immediately after impact, the change of diameter in all cases shows a similar behavior with no significant differences. On the other hand, during the contraction process, the maximum diameter shows differences. The droplet falling in the middle of the edge ($L_1 = 0$ mm) is the most widely spread, and the diameter is the smallest for the case of $L_1 =$

$+3$ mm due to the hindrance by the step edge. The time scale of spreading associated with inertia is approximately D_0/V which yields 1.0 millisecond for the experimental conditions. The maximum spreading occurs at the time of 3 or 4 times of this characteristic time.

3.2 Coalescence Experiments with a Stationary Droplet

Figures 8 through 10 show the behavior of coalescence between the impacting droplet and a stationary droplet as the impacting droplet spreads. For the case of $L_2 = 4.5$ mm (Fig. 8), the largest distance between the impacting and stationary droplets, the spreading process of the impacting droplet to the right side is disturbed, while the right

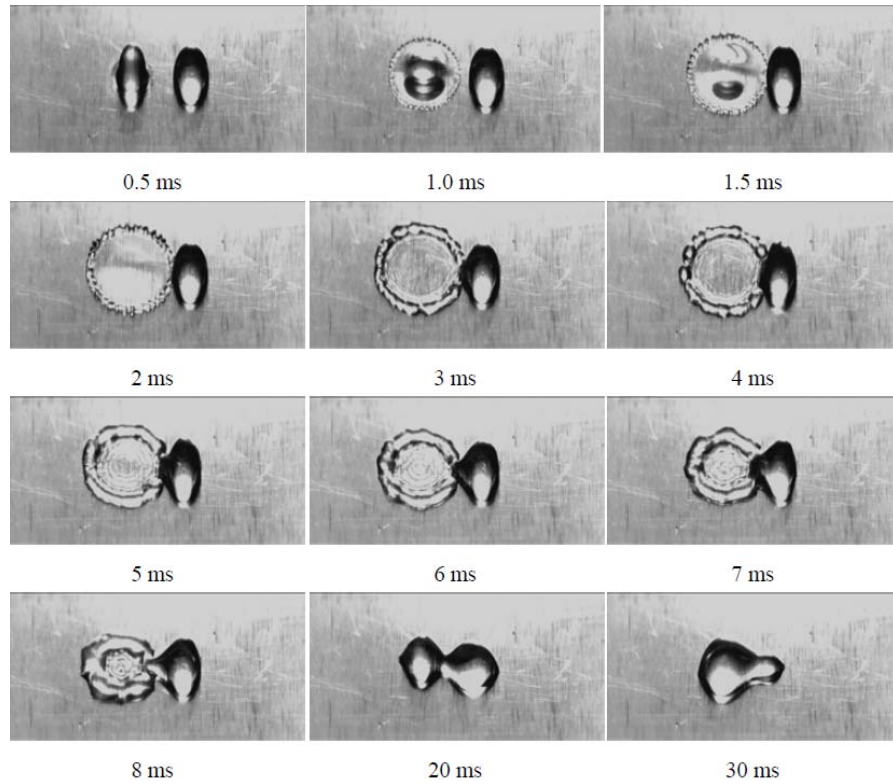


Fig. 8. The behavior of coalescence between the impacting droplet and a stationary droplet for distance of $L_2 = 4.5$ mm.

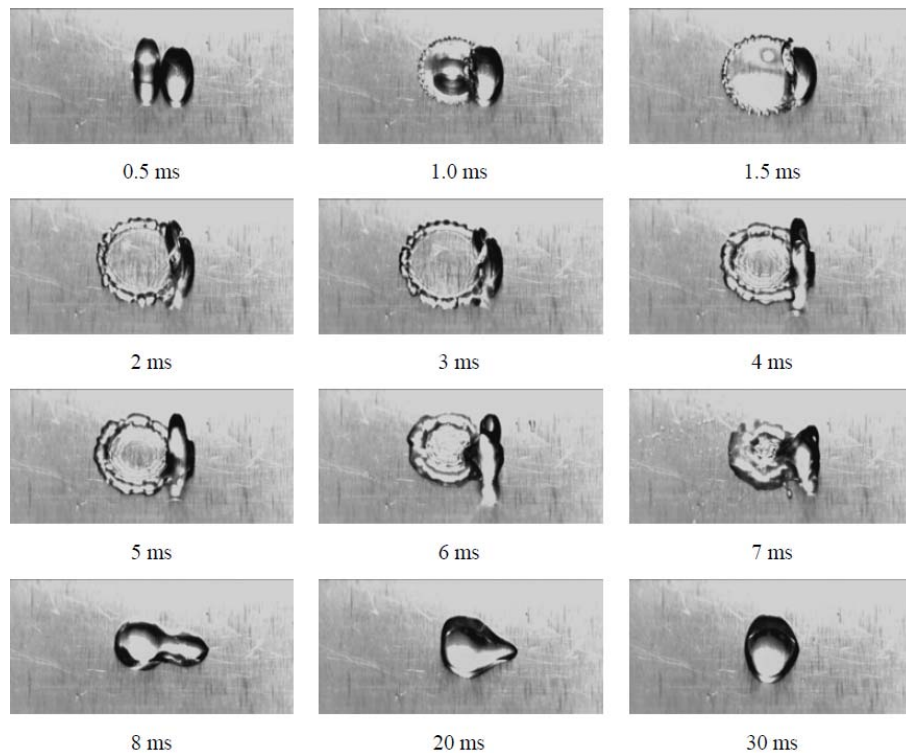


Fig. 9. The behavior of coalescence between the impacting droplet and a stationary droplet for distance of $L_2 = 3.0$ mm.

side of the spreading droplet coalesces with the stationary droplet. In the contraction process, the fluid inside the stationary droplet also moves to the impacting droplet. Eventually, the coalescing droplet shows the final shape with the left side

being larger because more fluid of the stationary droplet moved to the impacting droplet.

For the case of $L_2 = 3.0$ mm (Fig. 9), the fluid of the stationary droplet moves more toward the edge o

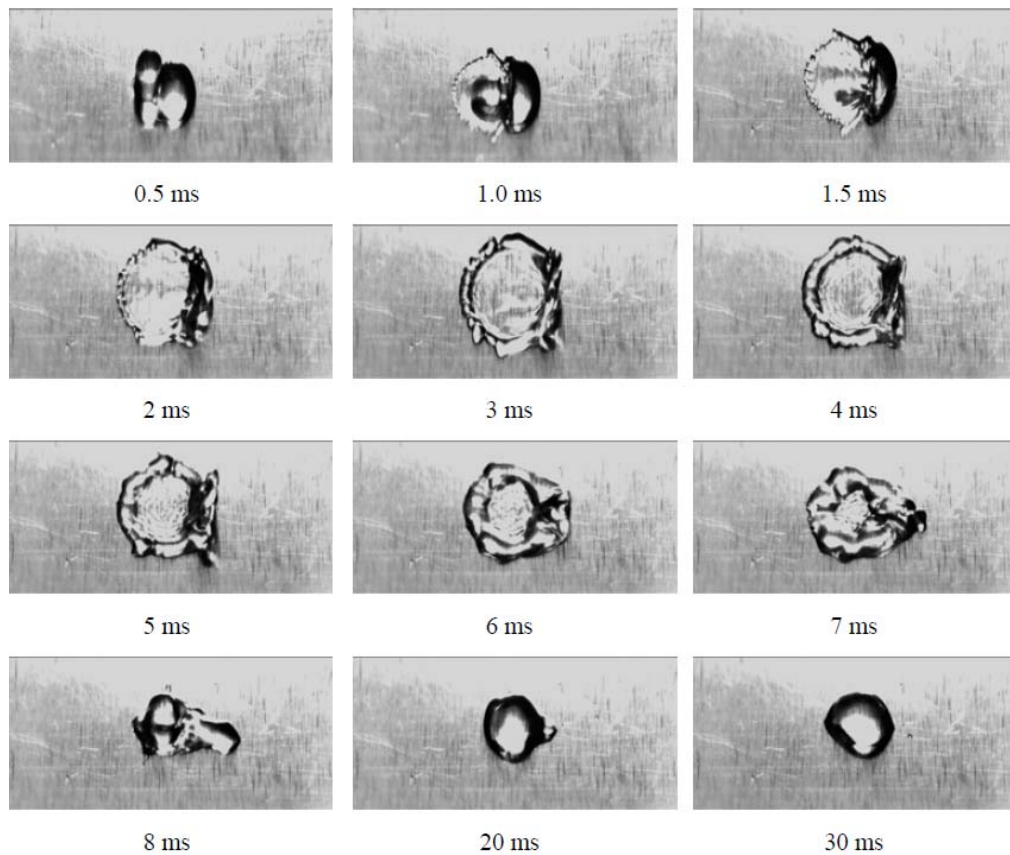


Fig. 10. The behavior of coalescence between the impacting droplet and a stationary droplet for distance of $L_2 = 1.5$ mm.

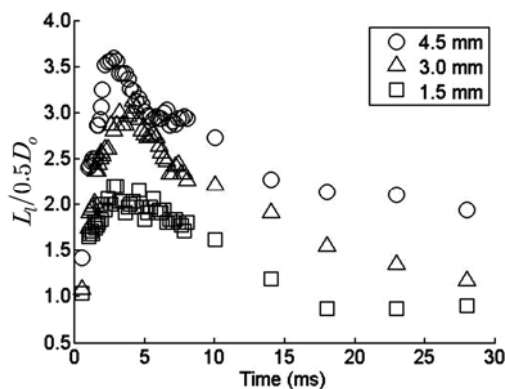


Fig. 11. The time history of the length from the center of the impacting droplet to the left side of the coalescing droplet.

f the spreading liquid film. Finally, the two droplets are completely coalesced because the flow of the stationary droplet to the left side is stronger, unlike in the previous case where a part of the stationary droplet remained in the final stage. If the distance between the liquid droplets decreases to the shortest distance ($L_2 = 1.5$ mm, Fig. 10), more flow from the stationary droplet moves to the impacting droplet. Most of the fluid of the stationary droplet merges with the impact droplet along the rim part of the liquid film, and then the coalescing droplet contracts to almost a single droplet.

Figure 11 shows the time history of the length from the center of the impacting droplet to the left side of

the coalescing droplet, L_t , which is nondimensionalized by the radius of the impacting droplet. The spreading in the left side of the impacting droplet is significantly influenced by the contact and coalescence with the stationary droplet. If the distance between the droplets is the farthest, they are spread by 3.5 times the radius of the impacting droplet, but in the case of the nearest distance, they are spread by only two times the radius of the impacting droplet. As the distance between the impact and stationary droplets becomes shorter, more fluid from the stationary droplet moves to the impact droplet along the circumference of the liquid film, so that spreading to the left side is much weakened.

Figure 12 shows the time history of the length from the center of the stationary droplet to the right side of the coalescing droplet, L_r , nondimensionalized by the radius of the stationary droplet. If the distance between the droplets is the farthest, there will not be much spreading to the right side because the kinetic energy of the impacting droplet is not transferred to the stationary droplet. In the case of the nearest distance, however, spreading to the right side is significantly increased due to the high transfer of the moving momentum from the impacting droplet to the stationary droplet.

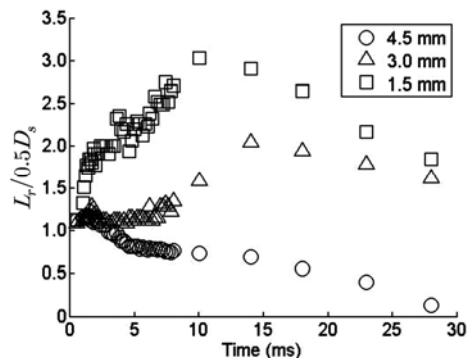


Fig. 12. The time history of the length from the center of the stationary droplet to the right side of the coalescing droplet.

Figure 13 shows the time history of the total length of the coalescing droplet, L_t , nondimensionalized by the distance between the droplets plus the radius of the impacting droplet and that of the stationary droplet. It can be seen that if the distance between the droplets is large, the droplets do not spread much because the small amount of kinetic energy transferred from the impacting droplet to the stationary droplet. When the distance between the droplets becomes small, more spreading occurs.

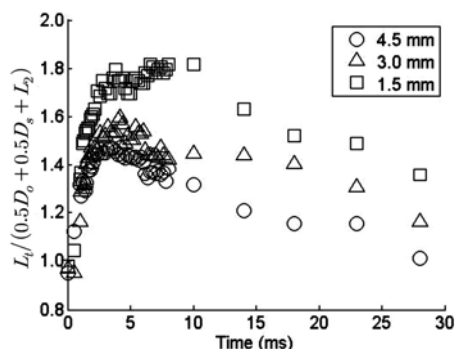


Fig. 13. The time history of the total length of the coalescing droplet.

5. CONCLUSION

In this study, we analyzed the effect of obstacles such as a step edge or a stationary droplet on the spreading-contraction process of the impacting droplet on a solid surface by visualizing the behavior of the impacting droplet with time delayed photography and measuring the diameter of the spreading-contraction droplets. In the experiments

with the step edge, the droplet falling in the middle of the edge was the most widely spread. If there was a wall on the left side of the impacting droplet, the climbing phenomenon appeared while the spreading was interrupted by the wall. As the distance between the stationary droplet and the impacting droplet was increased in the coalescence experiments with the stationary droplet, the left side of the coalescing droplet spread more than the right side because it could spread freely. The right side of the coalescing droplet spread more as the distance between two droplets became the smallest because more kinetic energy of the impacting droplet was transferred to the stationary droplet. The total length of the coalescing droplets, which combined the two effects, was the largest for the case in which the distance between the two droplets was the shortest.

REFERENCES

- Andrieu, C., D. Beysens, V. Nikolayev and Y. Pomeau (2002). Coalescence of sessile drops. *Journal of Fluid Mechanics* 453, 427-438.
- Bai, C. and A. Gosman (1995). Development of methodology for spray impingement simulation. *SAE Technical Paper* 950283.
- Bussmann, M., J. Mostaghimi and S. Chandra, (1999). On a three-dimensional volume tracking model of droplet impact. *Physics of Fluids* 11, 1406-1417.
- Chandra, S. and C. Avedisian (1991). On the collision of a droplet with a solid surface. *Proceedings of Royal Society of London, Series A* 432, 13-41.
- Crowe, C., M. Sommerfeld and Y. Tsuji (1998). *Multiphase flows with droplets and Particles*. CRC Press, Boca Raton.
- Jin, L., C. Yang, and K. Leong (2012). Dynamic behavior of liquid droplet impacting on heated surfaces. *Advances in Multiphase Flow and Heat Transfer* 4, 28-39.
- Josserand, C., L. Lemoyne, R. Troeger and S. Zaleski (2005). Droplet impact on a dry surface: triggering the splash with a small obstacle. *Journal of Fluid Mechanics* 52, 47-56.
- Lefebvre, A. (1989). *Atomization and Sprays*. Hemisphere, New York.
- Li, R., N. Ashgriz, S. Chandra, J. Andrews and S. Drappel (2010). Coalescence of two droplets impacting a solid surface. *Experiments in Fluids* 48, 1025-1035.
- Moreira, A., A. Moita and M. Pana (2010). Advances and challenges in explaining fuel spray impingement: How much of single

B. Kang/ JAFM, Vol. 8, No. 4, pp. 825-833, 2015.

droplet impact research is useful? *Progress in Energy and Combustion Science* 36, 554-580.

Menchaca-Rocha, A., A. Martinez-Davalos and R. Nunez (2001). Coalescence of liquid drops by surface tension. *Physical Review E* 63, 046309.

Mundo, C., M. Sommerfeld and C. Tropea (1995). Droplet-wall collisions: Experimental studies of the deformation and breakup process. *International Journal of Multiphase Flow* 21, 151-173.

Rein, M. (1993). Phenomena of liquid drop impact on solid and liquid surfaces. *Fluid Dynamics Research*, 12, 61-93.

Rioboo, R., M. Marengo and C. Tropea (2002). Time evolution of liquid drop impact onto solid, dry surfaces. *Experiments in Fluids* 33,

112-124.

Ristenpart, W., P. McCalla, R. Roy and H. Stone (2006). Coalescence of spreading droplets on a wettable substrate. *Physical Review Letters* 97, 064501.

Roisman, I., B. Prunet-Foch, C. Tropea and M. Vignes-Adler (2002). Multiple drop impact onto a dry solid substrate. *Journal of Colloid and Interface Science* 256, 396-410.

Thoroddsen, S., K. Takehara and T. Etoh (2005). The coalescence speed of a pendant and a sessile drop. *Journal of Fluid Mechanics* 527, 85-114.

Yarin, A. (2006). Drop impact dynamics: Splashing, spreading, receding, bouncing. *Annual Review of Fluid Mechanics* 38, 159-192.